Asian Journal of Chemistry; Vol. 25, No. 8 (2013), 4657-4660

ASIAN JOURNAL OF CHEMISTRY

http://dx.doi.org/10.14233/ajchem.2013.14439

Preparation of Ag-SiO_2 Nanocomposites and Photocatalytic Degradation of Organic Dyes

WEON BAE KO*, YOUN JUN OH and BUM HWI CHO

Department of Chemisty, Sahmyook University, Seoul 139-742, South Korea

*Corresponding author: Fax: +82 2 9795318; Tel: +82 2 33991700; E-mail: kowb@syu.ac.kr

(*Received*: 16 August 2012; *Accepted*: 18 February 2013) AJC-13036

Silicon dioxide (SiO_2) nanoparticles were synthesized using a sonochemical method by applying ultrasonic irradiation to a mixed aqueous-alcoholic solution of ammonium hydroxide with tetraethyl orthosilicate at room temperature. The morphology and optical properties of the Ag-SiO_2 nanocomposites were determined by X-ray diffraction, scanning electron microscopy, transmission electron microscopy and ultraviolet-visible spectroscopy. The Ag-SiO_2 nanocomposites were examined as a catalyst for the photocatalytic degradation of organic dyes, *e.g.*, methylene blue, methyl green, methyl violet, methyl orange and rhodamine B under visible light at 380-780 nm.

Key Words: SiO_2 nanoparticles, Ag nanoparticles, Ag-SiO_2 nanocomposites, Organic dyes, Photocatalytic degradation.

INTRODUCTION

Nanotechnology has been applied to the photooxidation of pollutants in waste water[1-7]. Nanocomposites are used widely for the photocatalytic splitting of water and the production of hydrogen[8-11]. Electrons in the conduction band and holes in the valence band are generated by the ultraviolet-visible light irradiation[12]. These can recombine in the bulk or move to the surface. Another key point factor that decreases the photocatalytic effect of nanocomposites is the high electron-hole recombination rate determined by time resolved spectroscopic studies[10]. The deposition of transition metal oxides or noble metals on the surface of a nanomaterial reduces the rate of electron-hole recombination because these deposits can capture the electrons in the conduction band or holes in the valence band[12]. This enhances the adsorption of the reactants and catalyzes reactions at the interface by transferring the holes or electrons to the adsorbed reactants[12]. The application of ultrasound has attracted the attention by some research groups as a synthetic process in chemistry because ultrasonic irradiation can cause chemical reactions either in heterogeneous or homogeneous systems[13,14]. The chemical reactions are promoted by the cavitation of a liquid caused by traveling ultrasonic waves. Here, cavitation suggests the formation of micro bubbles in a liquid subjected to sonication, which implode and generate high pressures and temperatures in their surroundings[13,14]. These nanocomposite materials have potential applications in a range of fields, such as surface-enhanced photonic crystals[15], catalysis[16,17], optics[18-23], biochemistry for chemical sensors[24] and antibacterial resources[25]. The distinctive optical properties of metal nanoparticles arise from the collective oscillation of conduction electrons upon an interaction with electromagnetic radiation *i.e.*, localized surface plasmon resonance (LSPR)[26]. The LSPR extinction spectrum is quite sensitive to the size, shape and local refractive index near the surface of the metal nanoparticles in addition to their inter particle distances, which is the basis of using LSPR as molecular sensing[27,28]. Most of nanostructures are made from noble metals, such as those of silver and gold nanoparticles[29-31]. These noble metal nanoparticles show an absorption band in the visible region (at 380-750 nm) by their LSPR. Silver nanoparticles show a plasmon resonance in the visible region and find even wider applications than gold[32]. This is because Ag is sensitive to the surrounding chemicals, causing oxidization and significant degradation of its plasmonic properties. In addition, in solution, Ag nanoparticles aggregate due to van der Waals forces[33]. To overcome these problems, Ag nanoparticles require application-specific coatings to passive or fuse the nanoparticle to the target molecules or surfaces[34]. The ideal coating should have multifunctional ability, a simple way to conjugate with the target molecules and the ability to adjust its morphology to control the degree to which the encapsulated nanoparticles interacts with its surrounding environment. Silica is an admirable candidate for such a generalized platform coating because it is chemically inert in a wide range of solvents, greatly transparent in the visible and IR regions of the spectrum and can be functionalized easily with silane coupling agents for further bio conjugation[35,36]. The silica shells (core-shell particles) not only improve the colloidal stability but also control the distance between the core particles within the

assemblies through the shell thickness[37-39]. In this paper, ultrasonic irradiation was used to synthesize silica-coated Ag nanoparticles (Ag@SiO_2) without an intermediate coating step. In addition, the photocatalytic activity of the Ag@SiO_2 nanocomposites in degrading organic dyes, such as methylene blue (MB), methyl green (MG), methyl violet (MV), methyl orange (MO) and rhodamine B (RhB) under visible light at 380-780 nm were investigated by ultraviolet-visible spectroscopy.

EXPERIMENTAL

Silver nitrate, ammonium hydroxide, tetraethyl orthosilicate, $NaBH_4$ and ethanol were supplied by Samchun Chemicals. The organic dyes (methylene blue, rhodamine B, methyl violet, methyl orange, and methyl green) were purchased from Sigma-Aldrich.

Silica nanoparticles, Ag nanoparticles and Ag-SiO_2 nanocomposites were prepared by ultrasonic irradiation using an ultrasonic generator (UGI1200, Hanil Ultrasonic Co., Ltd.) with a frequency 20 kHz and a nominal power of 750 W. The ultrasonic generator was a horn type system with a horn tip diameter of 13 mm.

Ag-SiO_2 nanocomposites were observed by scanning electron microscopy (SEM, Hitachi S4700) at an accelerating voltage of 0.5-15.0 kV. The morphology and crystallite size of the samples were examined by transmission electron microscopy (TEM, JEOL Ltd, JEM-2010) at an acceleration voltage of 200 kV. The structure of the nanomaterials (SiO_2 nanoparticles, Ag nanoparticles and Ag-SiO_2 nanocomposites) was examined by X-ray diffraction (XRD, Rigaku, Rigaku DMAX PSPC MDG 2000). The UV-visible spectra of the samples were observed using a UV-visible spectrophotometer (Shimazu UV -1691PC).

Synthesis of Ag-SiO_2 nanocomposites under ultrasonic irradiation: 4 mL of tetraethyl orthosilicate mixed with 3 mL of ammonium hydroxide in 50 mL of ethanol were exposed to ultrasonic conditions for 0.5 h. After ultrasonic irradiation, 10 mg (170 mM) of $AgNO_3$ and 1 mg (17 mM) of $NaBH_4$ were added to the mixed solution under ultrasonic irradiation for 1 h.

To obtain the Ag-SiO_2 nanocomposites, the mixed solution was centrifuged and the precipitated product was washed 4 times with mixed solvent (distilled water:ethanol = 1:1) and dried for 6 h at room temperature.

Degradation of various organic dyes with Ag-SiO_2 nanocomposites: The photocatalytic activities of the Ag-SiO_2 nanocomposites were evaluated with various organic dyes, such as methyl green, methylene blue, methyl violet, methyl orange, and rhodamine B, using UV-visible spectrophotometer under visible light at 380-780 nm. Before evaluating the photocatalytic activities of the photocatalysts, 0.01 mM of various organic dyes were dissolved in 100 mL of water and a 10 mL of the solution was placed into a vial and 10 mg of each photocatalyst was added separately to each these vials. The various organic dyes degraded by the photocatalyst under visible light at 380-780 nm were monitored by UV-visible spectrophotometer.

RESULTS AND DISCUSSION

Fig. 1 showed a SEM image of the Ag-SiO_2 nanocomposites. The Ag-SiO_2 nanocomposites contained Ag nanoparticles on the SiO_2 particle and the shape of Ag-SiO_2 was a quasi-sphere type. Fig. 2 showed a TEM image of Ag-SiO_2 nanocomposites. The Ag nanoparticles located on the SiO_2 surface were less than 5 nm in size. Fig. 3 showed XRD patterns of the Ag-SiO_2 nanocomposites. The peaks of the Ag-SiO_2 nanocomposites in the XRD patterns were observed at 38.08º(111), 44.28º(200), 64.24º(220) and 77.41º as a 2θ (311). Fig. 4 showed the UV-visible spectrum of the Ag-SiO_2 nanocomposites. The peak in the UV-visible spectrum was observed at 392 nm and was assigned to the surface plasmon resonance of silver nanoparticles. Fig. 5 shows the UV-visible spectra of the degraded organic dyes (methylene blue, methyl green, methyl violet, methyl orange, and rhodamine B) with Ag-SiO_2 nanocomposites under visible light at 380-780 nm. The Ag-SiO_2 nanocomposites showed effective photocatalytic activity in degrading the organic dyes (methylene blue, methyl violet, methyl green). The photocatalytic effect of the Ag-SiO_2 nanocomposites was more effective on methylene blue among the various organic dyes (methylene blue, methyl violet, and methyl green, methyl organe and rhodamine B) in the presence of visible light.

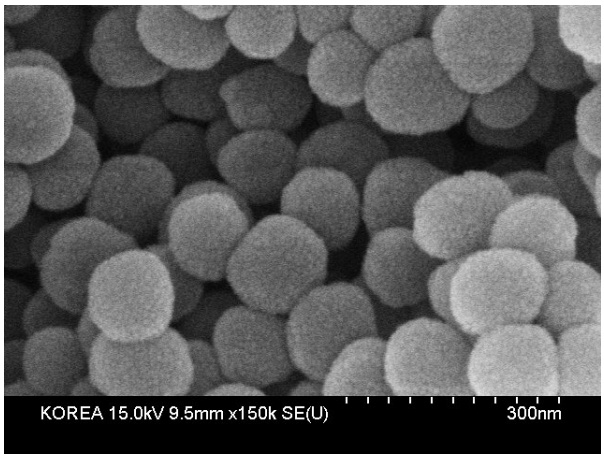

Fig. 1. SEM images of Ag-SiO_2 nanocomposites

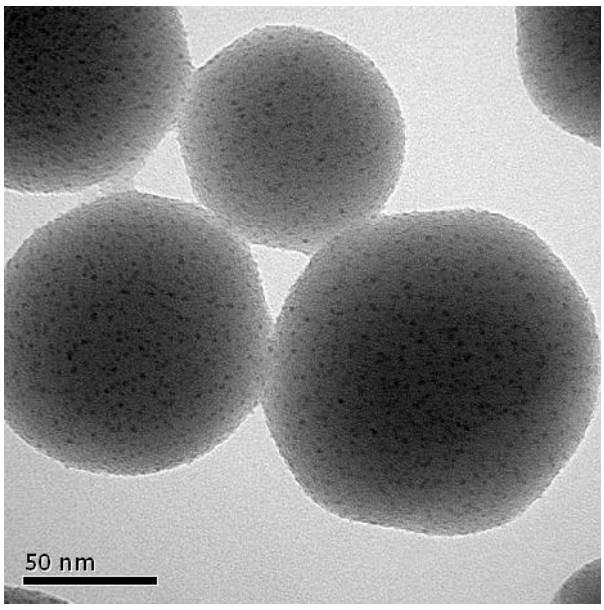

Fig. 2. TEM images of Ag-SiO_2 nanocomposites

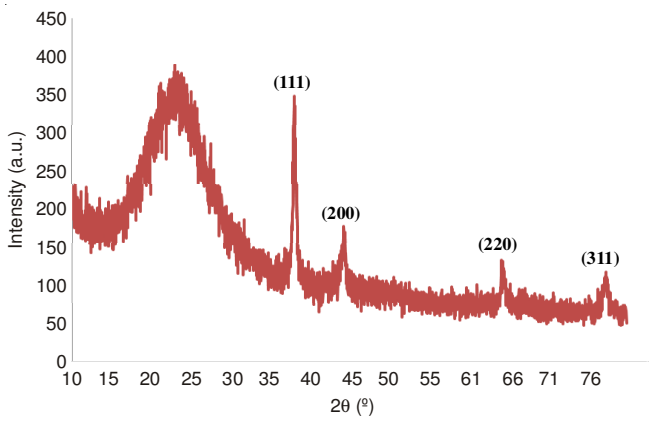

Fig. 3. XRD images of Ag-SiO_2 nanocomposites

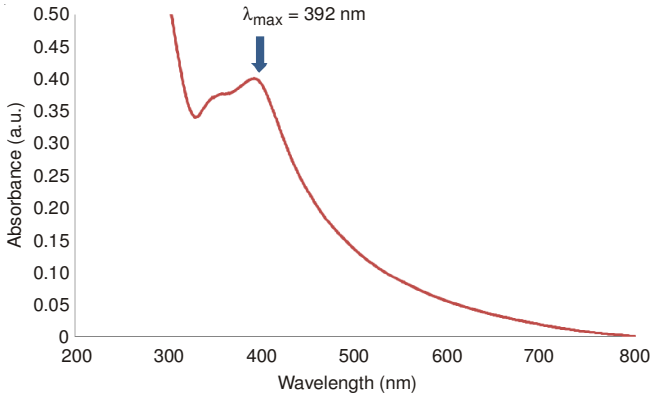

Fig. 4. UV-visible spectra of Ag-SiO_2 nanocomposites

Conclusion

This paper described the synthesis of Ag-SiO_2 nanocomposites by ultrasonic irradiation. The properties of Ag-SiO_2 nanocomposites were characterized by UV-visible, XRD, SEM and TEM. The Ag-SiO_2 nanocomposites used as a photocatalyst to evaluate the photocatalytic activity in various organic dyes

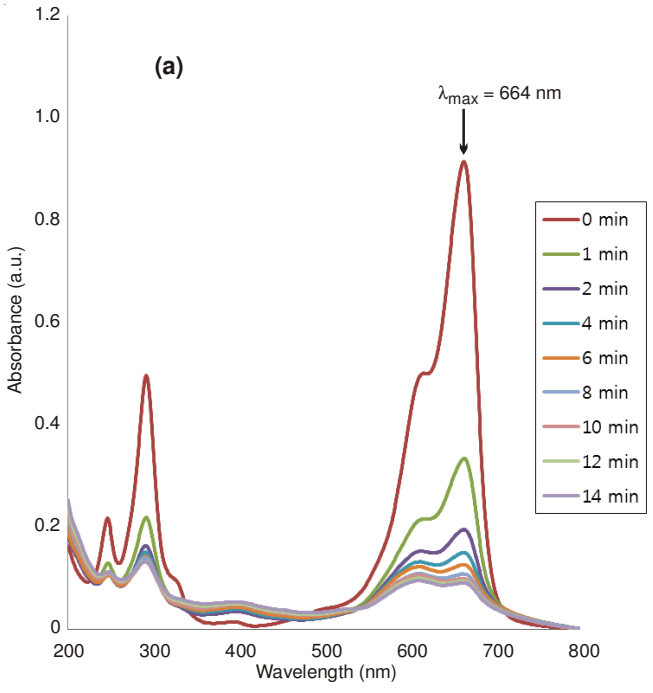

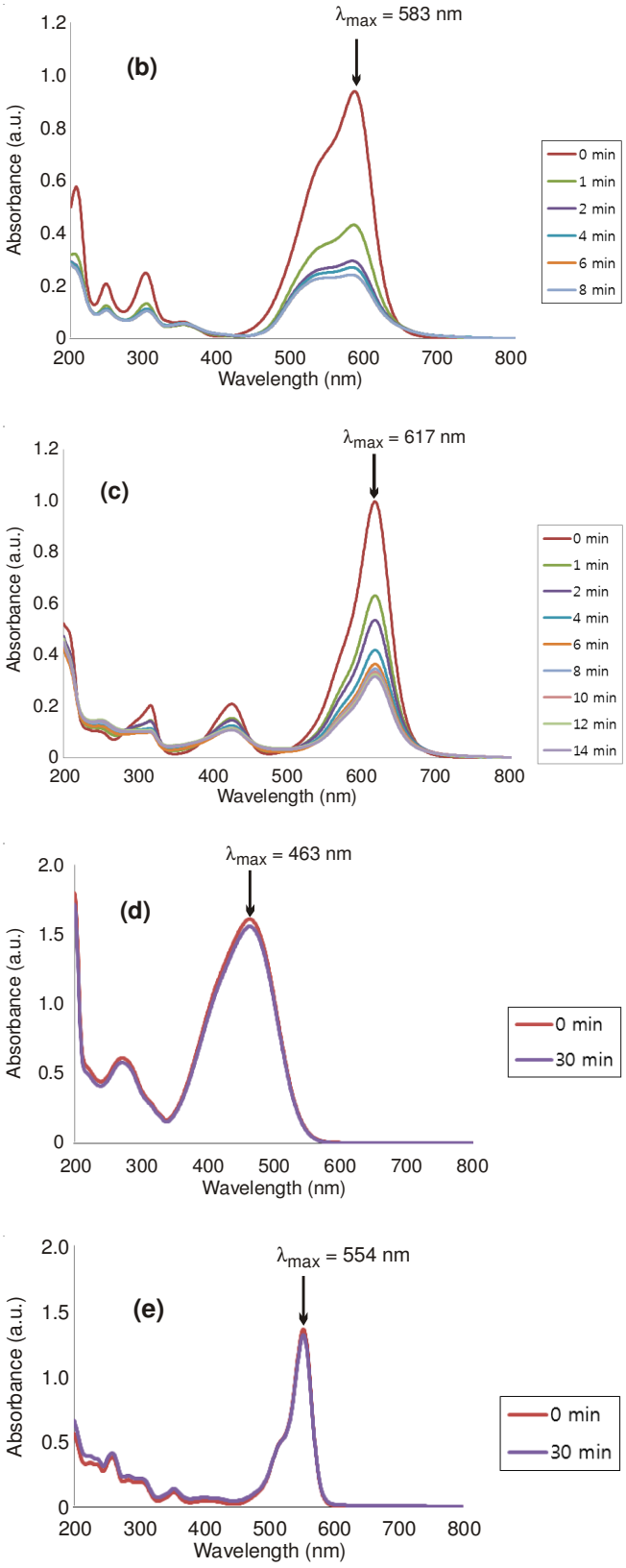

Fig. 5. UV-visible spectra of the degradation in (a) methylene blue, (b) methyl violet, (c) methyl green, (d) methyl orange and (e) rhodamine B with Ag-SiO_2 nanocomposites under visible-light at 380-780 nm

under visible ranges at 380-780 nm. UV-visible spectrophotometer was used to measure the concentration of organic dyes degraded by the photocatalyst and visible light. The Ag-SiO_2 nanocomposites as a photocatalyst were applied to the degra-

dation of various organic dyes, such as methyl green, methylene blue, methyl violet, methyl orange, and rhodamine B, under visible-light. Further studies of these nanomaterials as a photocatalyst for the decontamination of wastewater are currently underway.

ACKNOWLEDGEMENTS

This study was supported by Sahmyook University funding in Korea and the Ministry of Knowledge and Economy.

REFERENCES

1. Nano-technology, Encyclopedia Britannica on-line.
2. I. Bilecka, P. Elser and M. Niederberger, *ACS Nano*, **3**, 467 (2009).
3. J.F. Zhu, Y.J. Zhu, M.G. Ma, L.X. Yang and L. Gao, *J. Phys. Chem. C*, **111**, 3920 (2007).
4. A.V. Murugan, C.W. Kwon, G. Campet, B.B. Kale, A.B. Mandale, S.R. Sainker, C.S. Gopinath and K. Vijayamohanan, *J. Phys. Chem. B*, **108**, 10736 (2004).
5. S. Galema, *Chem. Soc. Rev*., **26**, 233 (1997).
6. Z.L. Wang, C.T. Chan, W.Y. Zhang, Z. Chen, N.B. Ming and P. Sheng, *Phys. Rev. B*, **64**, 113108 (2001).
7. S. Nie and S.R. Emory, *Science*, **275**, 1102 (1997).
8. C.W. Chen, T. Serizawa and M. Akashi, *Chem. Mater*., **11**, 1381 (1999).
9. R. Narayanan and M.A. El-Sayed, *J. Phys. Chem. B*, **109**, 12663 (2005).
10. W.L. Barnes, A. Dereux and T.W. Ebbesen, *Nature*, **424**, 824 (2003).
11. R. Elghanian, J.J. Storhoff, R.C. Mucic, R.L. Letsinger and C.A. Mirkin, *Science*, **277**, 1078 (1997).
12. M.G. Cerruti, M. Sauthier, D. Leonard, D. Liu, G. Duscher, D.L. Feldheim and S. Franzen, *Anal. Chem*., **78**, 3282 (2006).
13. R.L. Stoermer, K.B. Cederquist, S.K. McFarland, M.Y. Sha, S.G. Penn and C.D. Keating, *J. Am. Chem. Soc*., **128**, 16892 (2006).
14. Y. Lu, G.L. Liu and L.P. Lee, *Nano Lett*., **5**, 5 (2005).
15. S.A. Kalele, S.S. Ashtaputre, N.Y. Hebalkar, S.W. Gosavi, D.N. Deobagkar, D.D. Deobagkar and S.K. Kulkarni, *Chem. Phys. Lett*., **404**, 136 (2005).
16. J.X. Wang, L.X. Wen, Z.H. Wang and J.F. Chen, *Mater. Chem. Phys*., **96**, 90 (2006).
17. S.K. Hong, G.Y. Yu, C.S. Lim and W.B. Ko, *Elast. Compos*., **45**, 206 (2010).
18. C. Noguez, *J. Phys. Chem. C*, **111**, 3806 (2007).
19. C. Wu and Q.H. Xu, *Langmuir*, **25**, 9441 (2009).
20. M.A. Martins, S. Fateixa, A.V. Girão, S.S. Pereira and T. Trindade, *Langmuir*, **109**, 4140 (2010).
21. C.R. Yonzon, D.A. Stuart, X. Zhang, A.D. McFarland, C.L. Haynes and R.P. VanDuyne, *Talanta*, **67**, 438 (2005).
22. J. Hu, Z. Wang and J. Li, *Sensors*, **7**, 3299 (2007).
23. L. Li, E.S.G. Choo, S. Tang, J. Ding and J. Xue, *Acta Mater*., **58**, 3825 (2010).
24. P. Mulvaney, *Langmuir*, **12**, 788 (1996).
25. T. Ung, L.M. Liz-Marzán and P. Mulvaney, *Langmuir*, **14**, 3740 (1998).
26. P.D. Cozzoli, T. Pellegrino and L. Manna, *Chem. Soc. Rev*., **35**, 1195 (2006).
27. I. Pastoriza-Santos, J. Perez-Juste and L.M. Liz-Marzán, *Chem. Mater*., **18**, 2465 (2006).
28. Y.D. Yin, Y. Lu, Y.G. Sun and Y.N. Xia, *Nano Lett*., **2**, 427 (2002).
29. L.M. Liz-Marzán, M. Giersig and P. Mulvaney, *Langmuir*, **12**, 4329 (1996).
30. T. Ung, L.M. Liz-Marzán and P. Mulvaney, *Langmuir*, **14**, 3740 (1998).
31. S.M. Marinakos, D.A. Shultz and D.L. Feldheim, *Adv. Mater*., **11**, 34 (1999).
32. V.V. Hardikar and E. Matijevic, *J. Colloid Interf. Sci*., **221**, 133 (2000).
33. S.R. Hall, S.A. Davis and S. Mann, *Langmuir*, **16**, 1454 (2000).
34. P. Mulvaney, L.M. Liz-Marzán, M. Giersig and T. Ung, *J. Mater. Chem*., **10**, 1259 (2000).
35. Y. Kobayashi, M.A. Correa-Duarte and L.M. Liz-Marzán, *Langmuir*, **17**, 6375 (2001).
36. G. Cho, B.M. Fung, D.T. Glatzhofer, J.-S. Lee and Y.-G. Shul, *Langmuir*, **17**, 456 (2001).
37. T. Tago, T. Hatsuta, R. Nagase, M. Kishida and K. Wakabayashi, *Kagaku Kogaku Ronbunshu Japanese*, **27**, 288 (2001).
38. H. Wang, H. Nakamura, Y. Yao, H. Maeda and E. Abe, *Chem. Lett*., **30**, 1168 (2001).
39. L.M. Liz-Marzán and P. Mulvaney, *J. Phys. Chem. B*, **107**, 7312 (2003).